This article was downloaded by: *[Syracuse University]*
On: *26 October 2009*
Access details: *Access Details: [subscription number 915950213]*
Publisher *Taylor & Francis*
Informa Ltd Registered in England and Wales Registered Number: 1072954 Registered office: Mortimer House, 37-41 Mortimer Street, London W1T 3JH, UK

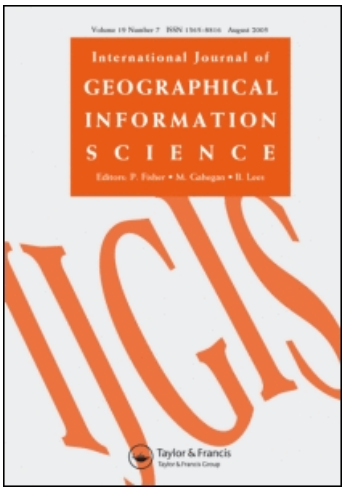

International Journal of Geographical Information Science
Publication details, including instructions for authors and subscription information:
http://www.informaworld.com/smpp/title~content=t713599799

Multi-scale spatiotemporal analyses of moose-vehicle collisions: a case study in northern Vermont

Giorgos Mountrakis [a]; Kari Gunson [b]
[a] Department of Environmental Resources and Forest Engineering, College of Environmental Science and Forestry, State University of New York, Syracuse, NY 13210, USA [b] Eco-Kare International, Toronto, Ontario, Canada M4E 1C0

Online Publication Date: 01 November 2009

To cite this Article Mountrakis, Giorgos and Gunson, Kari(2009)'Multi-scale spatiotemporal analyses of moose-vehicle collisions: a case study in northern Vermont',International Journal of Geographical Information Science,23:11,1389 — 1412
To link to this Article: DOI: 10.1080/13658810802406132
URL: http://dx.doi.org/10.1080/13658810802406132

PLEASE SCROLL DOWN FOR ARTICLE

Full terms and conditions of use: http://www.informaworld.com/terms-and-conditions-of-access.pdf

This article may be used for research, teaching and private study purposes. Any substantial or systematic reproduction, re-distribution, re-selling, loan or sub-licensing, systematic supply or distribution in any form to anyone is expressly forbidden.

The publisher does not give any warranty express or implied or make any representation that the contents will be complete or accurate or up to date. The accuracy of any instructions, formulae and drug doses should be independently verified with primary sources. The publisher shall not be liable for any loss, actions, claims, proceedings, demand or costs or damages whatsoever or howsoever caused arising directly or indirectly in connection with or arising out of the use of this material.

International Journal of Geographical Information Science
Vol. 23, No. 11, November 2009, 1389–1412

Taylor & Francis
Taylor & Francis Group

Research Article

Multi-scale spatiotemporal analyses of moose–vehicle collisions: a case study in northern Vermont

GIORGOS MOUNTRAKIS† and KARI GUNSON*‡

†Department of Environmental Resources and Forest Engineering, College of Environmental Science and Forestry, State University of New York, 419 Baker Hall, 1 Forestry Dr, Syracuse, NY 13210, USA

‡Eco-Kare International, P.O. Box 51522, Toronto, Ontario, Canada M4E 1C0

(*Received 29 February 2008; in final form 28 July 2008*)

Downloaded By: [Syracuse University] At: 19:35 26 October 2009

Moose–vehicle collisions (MVCs) pose a serious safety and environmental concern in many regions of Europe and North America. For example, in the state of Vermont, one-third of all reported MVCs resulted in motorist injury or fatality while collisions have increased from two in 1982 to 164 in 2002. Our work used a MVC dataset from 1983 to 1999 in the Northeastern Highlands of Vermont (four major roads) to perform space, time and spatiotemporal analyses and guide future mitigation strategies. An adapted kernel density estimator was implemented for exploratory analyses to detect high density collision hotspots on roads. The kernel in space showed seven major density peaks which varied in magnitude and spread between roads. The kernel estimator in time for all roads showed an exponentially increasing trend with annual periodicity and a seasonal cyclic component, where the majority of collisions occurred from May to October. Spatiotemporal kernel estimation exhibited discontinuous density hotspots in time and space suggesting changing animal movement patterns across roads. We used an adapted Ripley's *K*-function to test the hypothesis that MVCs clustering occurred at multiple scales in space, in time and in space–time combined. Statistically significant spatial clustering was evident on all roads at spatial scales from 2 to 10 km. A more consistent clustering in time occurred on all roads at a scale distance of 5 years. Similar to the kernel estimation, annual periodicity was also evident. Positive space–time clustering was present at small spatial (5 km) and temporal scales (2 years) indicating that where MVCs occur is also influenced by when they occur. In retrospect, using multiple road lengths, and the combined kernel estimation and Ripley's *K*-function in time and space, provided a powerful methodology to study varying spatiotemporal patterns of wildlife collisions along roads. This can greatly assist transportation planners in identifying optimal mitigation strategies along specific roads, such as deciding on location and spatial length for permanent and expensive measures (e.g. crossing structures and associated fencing) versus less permanent and inexpensive structures (e.g. wildlife signage and reduced speed limits).

Keywords: Spatiotemporal; Wildlife-vehicle collisions; Kernel; Ripley's *K*; Moose; Vermont

*Corresponding author. Email: kegunson@eco-kare.com

International Journal of Geographical Information Science
ISSN 1365-8816 print/ISSN 1362-3087 online © 2009 Taylor & Francis
http://www.tandf.co.uk/journals
DOI: 10.1080/13658810802406132

1. Introduction

1.1 *Problem statement and research questions*

Over the past few decades, vehicle collisions with animals have increased substantially in Europe and North America (Groot and Hazebroek 1996, Romin and Bissonette 1996, Seiler 2005) mostly due to increasing traffic volumes and animal population sizes (Hubbard *et al.* 2000, Seiler 2004). These collisions pose serious issues for transportation and wildlife agencies responsible for traffic safety, socioeconomic impacts, animal welfare, and wildlife management and conservation (Groot and Hazebroek 1996, Romin and Bissonette 1996, Schwabe *et al.* 2002). For example, in 2001, the costs attributed to vehicle collisions with moose in Newfoundland, Canada (e.g. health care and vehicle damage costs) have been reported upwards of CAN$1,200,000 (Joyce and Mahoney 2001).

In regions where collisions with large animals such as moose are prevalent, human safety becomes a prominent issue, in addition to the loss in wildlife population numbers. Moose are of particular concern for motorist safety because their tall stature (upward of 9 feet tall) can cause intrusion into the passenger compartment of vehicles, and their heavy weight (over 1000 pounds) causes the greatest vehicle damage, personal injury and human death compared to collisions with any other animal (Maine Department of Transportation 2001). For example, in Maine, one out of four reported moose collisions results in serious injuries or death for humans (Maine Department of Transportation 2001) and in Sweden, between 10 and 15 motorists are involved in a fatal collision with moose annually (Seiler 2004). In Vermont, reported traffic statistics from 2002 to 2005 showed 33% of all moose–vehicle collisions (MVCs) resulted in injury or fatality as compared to only 7% with deer–vehicle collisions (Vermont Department of Transportation, personal communication).

A variety of road mitigation strategies, such as the use of fencing, wildlife crossing structures and wildlife crossing signs, have been implemented by transportation and natural resource agencies to reduce road-related wildlife mortality (Romin and Bissonette 1996, Clevenger and Waltho 2000, Krisp and Durot 2007, Huijser *et al.* 2007). The implementation of wildlife crossing structures embedded in the road network is a relatively expensive and permanent measure. For example, crossing structure installation in Banff National Park varied from CAN $250,000 to $1,750,000 for underpasses and overpasses respectively, and can vary depending on the dimensions, materials and surrounding landscape characteristics (Mcguire and Morrall 2000). Also, crossing structures can have a life span of up to 80 years (Huijser *et al.* 2007). Typically, there are limited funds for research conducted to provide justification for costly mitigation leading to the implementation of relatively less permanent and inexpensive measures, such as seasonal wildlife signage, reduced speed limits, wildlife warning reflectors and public awareness programs (Romin and Bissonette 1996, D'Angelo *et al.* 2006, Huijser *et al.* 2007).

Motivated by the complexity of providing economical and effective mitigation strategies, we developed two main objectives for this study:

- develop a multi-scale space, time and spatiotemporal methodology for analyzing point data (events) along one-dimensional spatial features (e.g. roads). This will also include a statistical approach which tests the null hypothesis that MVCs are not clustered in space, time or space and time combined.

Downloaded By: [Syracuse University] At: 19:35 26 October 2009

- provide a case study implementing our methodology to determine spatiotemporal patterns for MVCs in Vermont and subsequently assist transportation planners in determining appropriate mitigation measures.

For the remainder of the introduction, we describe the study area, the MVC dataset and some initial exploratory investigations of the dataset. Section 2 describes the algorithms used, Kernel estimation and Ripley's *K*-function, and their related applications. In Sections 3 and 4, we provide the results and discussion for each algorithm respectively. In Section 5, we compare the results obtained from the two algorithms and discuss the results as they pertain to transportation mitigation. In Section 6, we draw conclusions, followed by logical choices for future work derived from our analyses (Section 7).

1.2 *Study area and preliminary investigations*

Downloaded By: [Syracuse University] At: 19:35 26 October 2009

Our study area (Figure 1) was within the state of Vermont, which consists of eight biophysical ecoregions (Thompson 2002). We specifically selected the northeastern highlands (approximately 2178 km^2 or 10% of the state) to perform our analyses, because 33% of all the MVCs were concentrated in this region. We selected three major routes, VT-114, US-2 and VT-105, where 68% of the reported MVCs in the highlands occurred. The MVC mortality rate was substantially different between the northern and southern sections of VT-114 separated by VT-105; therefore, this highway was divided into VT-114N and VT-114S for all further analyses. The frequency of annual moose collisions in the NH increased from zero in 1980 to just over 200 in 1997, in response to a population expansion of moose from 200 in 1980 to over 4500 moose in 2006 (Vermont Department of Fish and Wildlife 1998).

The highlands region is part of a much larger boreal ecosystem which extends into the north and east. Vegetation consists of broad-scale patterns of natural northern hardwoods, spruce and fir, and large softwood swamps and bogs (Thompson 2002). The terrain is at a higher elevation (494 m) relative to the entire state average at 355 m. Since 43 per cent of the region is protected from development, human settlement is low, i.e. 3.68 dwellings/km^2 as compared to 12.09 dwellings/km^2 statewide [Vermont Centre for Geographic Information (VCGI), http://www.vcgi.org]. Annual average daily traffic volumes (AADTV) is 1128 vehicles as measured from 103 automated traffic counters from 1975 to 2003 in the highlands [Vermont Agency of Transportation (VAOT), http://www.vcgi.org]. Road density (all state highways, town and private roads) in this region is lower (0.85 km road/km^2) compared to the state mean of 1.27 km road/km^2.

Collision data for the entire province (1488 MVCs) had been recorded in the state police system from 1983 to 2005 by highway maintenance personnel, state game wardens and wildlife biologists (Austin *et al.* 2006). Location data were originally recorded in various formats such as the distance from a road intersection, landmark or road marker, and coordinates were later attached to each collision record (Austin *et al.* 2006). Though most have much better accuracy, records included in this database have spatial error up to 800 m (Austin *et al.* 2006). The temporal resolution of the dataset included day, month and year for each collision. Our temporal analyses were performed in monthly intervals, so possible reporting errors of ± 1 day did not affect our analyses. We should also note that our analyses are based on recorded incidents which are conservative because it does not include unreported cases or when animals die away from the road.

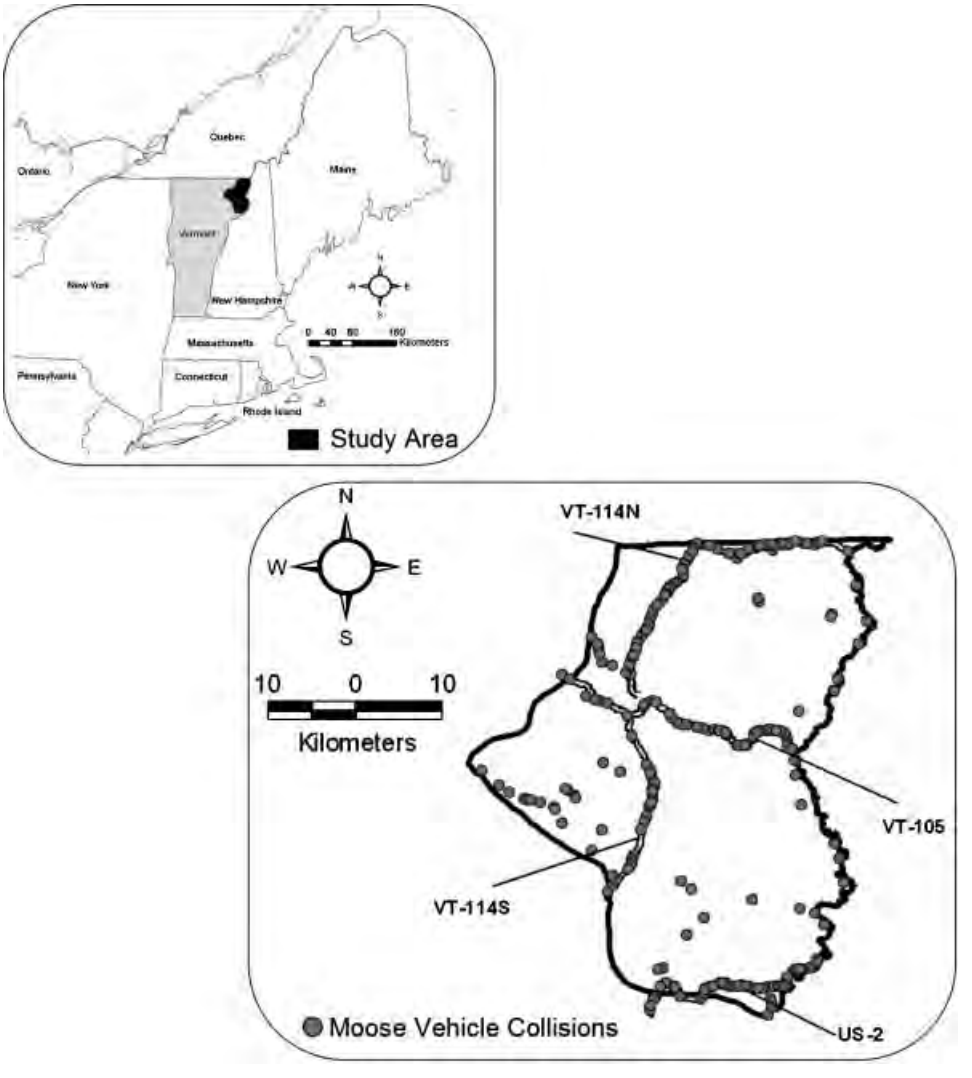

Figure 1. Map of our study area: the bold region represents the northeastern highlands of Vermont (top left). Magnification of the highlands with moose vehicle collision data overlaid on the selected roads (bottom right).

Visual inspection of Figure 1 shows that MVCs in the highlands region are not random occurrences, but are clustered to specific road segments, which motivated us to further investigate the distribution of MVCs using spatial statistics. We also plotted MVCs by month (Figure 2) and year (Figure 3) to determine the general seasonal and annual trends in the temporal dimension. The monthly summary showed clustering of MVCs during the summer months when animals are most active.

Collision data in the NH followed a consistent increasing trend, from 1983 to 1996 (Figure 3). Collisions fluctuated from 1997 to 1999 and there was a dramatic decline in MVCs post-1999. This can be attributed to a combination of increased hunting, a decrease in sampling effort and a time lag for data input into the database (VAOT, personal communication). In order to compare MVCs in a consistent manner, we used data from 1983 to 1999 (total of 438 MVCs) for all further

Downloaded By: [Syracuse University] At: 19:35 26 October 2009

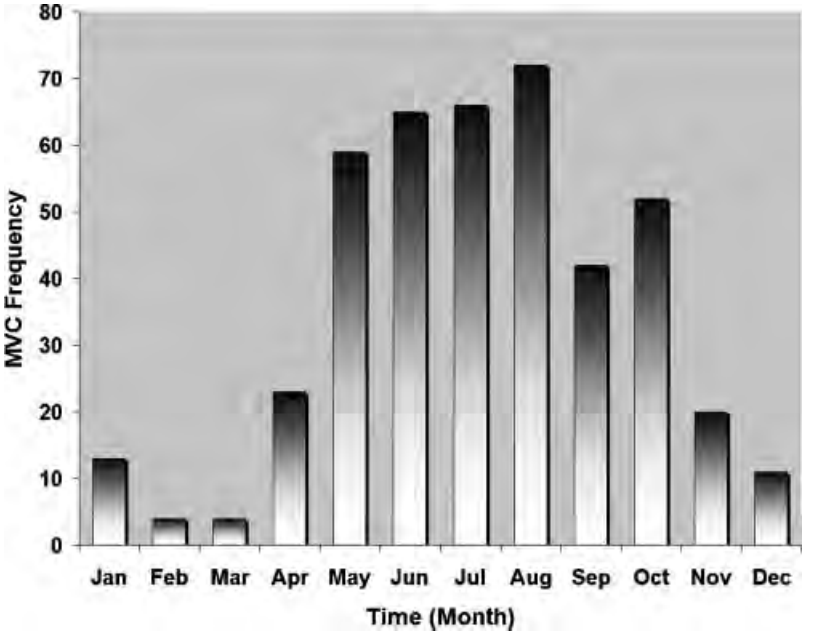

Figure 2. Monthly frequency of moose-vehicle collisions in the Northeastern Highlands of Vermont from 1983 to 2006.

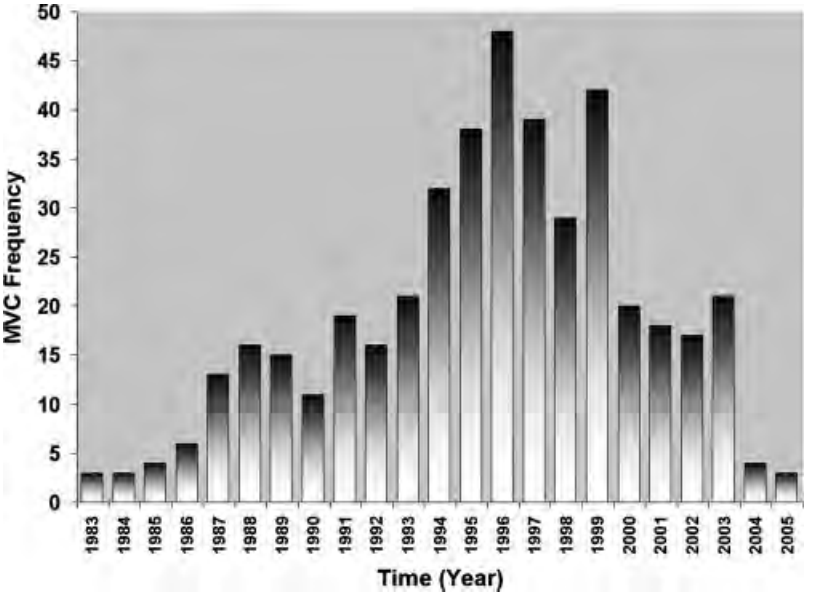

Figure 3. Yearly frequency of moose-vehicle collisions in the Northeastern Highlands of Vermont from 1983 to 2006.

spatiotemporal analyses. We should note that the two-dimensional spatial coordinates were combined into a one-dimensional attribute expressing road length, a valid generalization since the examined roads were high-speed roads without significant sharp turns. If numerous sharp turns exist, then the two-dimensional Euclidean distances would be smaller than the one-dimensional road length

Downloaded By: [Syracuse University] At: 19:35 26 October 2009

distances leading to different clustering scales. Additionally, our analyses assume the same distribution of road traffic on all roads and do not take into account varying traffic patterns related to one-way roads or extreme events (e.g. high summer seasonal traffic). We used Matlab v7.1 and ArcView 9.1 software programming packages for all exploratory and statistical analyses (Environmental System Research Institute 2005; Mathworks 2005).

2. Methodology and existing approaches

2.1 *Kernel estimation*

The kernel estimation is not a statistical method to quantify clustering; instead, it generates comparable distribution maps of density. The density is calculated using a moving window; points closest to the window's center (cell center) contribute most to the calculated index of density (Bastin *et al.* 2006). In our case, we adapted the kernel estimation equation as described by Bailey and Gatrell (1995) to generate one-dimensional cell centers along a road, therefore measuring density per unit length, not area. We also implemented the two-dimensional kernel estimation to explore space–time interactions.

In our case, the kernel density is calculated using a one-dimensional distance h_i, representing the one-dimensional distance between the center of the kernel and a collision point p (equation (1)). The contribution of a point depends on the distance to the kernel center h_i reaching a maximum at distance zero and a minimum at a user-defined kernel bandwidth distance τ. For the space–time interaction kernel, the two densities, one for space and one for time, were then added together to obtain a combined density measure for each space–time cell center.

$$\lambda_\tau(p) = \sum_{h_i < \tau} \frac{1}{2\tau}\left(1 - \frac{h_i^2}{\tau^2}\right) \tag{1}$$

The kernel estimation is highly sensitive to the bandwidth or smoothing factor because it determines the search radius or in our case the search length in which events will contribute to the density at each MVC (Bailey and Gatrell 1995). If the bandwidth is too large, local densities will be obscured and become similar to the density of the entire study area; if it is too small, the density will be a collection of spikes centered at each event. A balance must be achieved between displaying too much noise and 'spikes' in the data, and obliterating important local variation altogether (Bastin *et al.* 2007). Experimentation is required to select the optimal bandwidth, which meet the objectives of each study (Krisp and Durot 2007, Gitzen *et al.* 2006, Bastin *et al.* 2006). In our analyses, we varied the bandwidth within a range relevant to transportation mitigation planning.

2.2 *Ripley's K-function*

The Ripley's *K*-function (Ripley 1976, 1981) or reduced second moment function, measures spatial dependence or clustering of events at multiple scales. It is a widely accepted tool for analyzing spatial point patterns; however, its use for analysis of temporal point patterns is not as well documented (Diggle *et al.* 1995). Observed distributions can be compared to random distributions to determine the distance where clustering becomes

Downloaded By: [Syracuse University] At: 19:35 26 October 2009

significant. It is advantageous with respect to the nearest neighbor distance methods because it examines spatial relationships between all points at different scales.

2.2.1 Univariate Ripley's K-function applied separately in space or time. We first calculated the one-dimensional distance between all possible MVCs in space (km) or time (month) (d_{ij} and t_{ij} respectively) along a single dimension (equations (2) and (3)). We also defined a scale distance for space (s) and time (t) that increased in equal increments for each iteration of the algorithm. We then used the K-function at every MVC to count the number of MVCs within the specified scale distance ($d_{ij}<s$ or $t_{ij}<t$); the indicator function (I) codes points within that distance as 1, and 0 otherwise. The algorithm then sums the coded 1s ($\Sigma\Sigma$) for every MVC. This process continues for each scale distance until the maximum distance is reached. The final count is then normalized by road or time length (RL or TL) and the number of non-self pairs $[n(n-1)]$ (equations (2) and (3)). We compared the observed K intensity for each temporal or spatial length to the expected intensity at each length in a random process, thus providing a one-dimensional representation for the L-function, (equations (4) and (5)), adapted from the L function for a two-dimensional area (Bailey and Gatrell 1995). For a random distribution $L=0$, peaks in positive values tend to indicate clustering while troughs of negative values indicate regularity at each corresponding scale distance.

$$K(s) = \sum \sum_{i \neq j} I_s(d_{ij}) \mathrm{RL} / [n(n-1)] \tag{2}$$

$$K(t) = \sum \sum_{i \neq j} I_t(t_{ij}) \mathrm{TL} / [n(n-1)] \tag{3}$$

$$L(s) = \frac{K(s)}{2} - s \tag{4}$$

$$L(t) = \frac{K(t)}{2} - t \tag{5}$$

2.2.2 Bivariate K-function: spatiotemporal analysis. We calculated the space–time interaction function $K(s, t)$ by counting the number of MVCs within each spatial distance (s) and time interval (t) and scaling it by the expected number of MVCs per unit area and per unit time (equation (6)). If the processes operating in time and space are independent (no space-time interaction) then $K(s,t)$ should be the product of the two K-functions, one in space $K(s)$ and the other in time $K(t)$ (Bailey and Gatrell 1995, Diggle *et al.* 1995). The $D(s, t)$ statistic measures the difference between $K(s,t)$ and $K(s)K(t)$ (equation (7)), at every combination of s and t to measure additional clustering due to the space–time interaction. Since the useful information in $D(s,t)$ is confined to values of s and t which are small relative to the spatial and temporal dimensions, we used a normalized index $D_o(s, t)$ (equation (8)). This index measures the proportional excess or increased risk due to space–time interaction and decreases for sufficiently large scale distances (Diggle *et al.* 1995). Both statistics have expected values of zero under a null hypothesis of space–time independence. If there is evidence of a space–time interaction for MVCs, there will be positive or raised values of $D(s, t)$ and $D_o(s, t)$ (at smaller magnitude).

Downloaded By: [Syracuse University] At: 19:35 26 October 2009

$$K(s, t) = \sum \sum_{i \neq j} I_s(d_{ij}) I_t(t_{ij}) \mathrm{RLTL} / [n(n-1)] \quad (6)$$

$$D(s, t) = K(s, t) - K(s)K(t) \quad (7)$$

$$D_o(s, t) = D(s, t) / K(s)K(t) \quad (8)$$

2.3 *Related approaches*

Kernel density algorithms provide a smooth density measure for spatial point patterns and have been used by epidemiologists to find geographical hotspots of disease (Bastin *et al.* 2007), transportation planners to determine the density of vehicle crashes along roads (Steenberghen *et al.* 2004), wildlife biologists to quantify home ranges from high density telemetry points (Moser and Garton 2007, Fieberg 2007), and road ecologists to identify hotspots of wildlife–vehicle collisions along roads (Ramp *et al.* 2005, 2006, Krisp and Durot 2007). Sauer *et al.* (1999) adjusted the algorithm to measure the magnitude of events per unit length (i.e. one-dimensional space), and Levine (2005) has adapted the algorithm to measure bivariate space and time data in a two-dimensional area. In our case study, we use kernel estimation to measure univariate space and time, and bivariate space and time densities of MVCs along road lengths.

Similar to the kernel estimator, the Ripley's *K*-function (Ripley 1976, 1981), which estimates spatial clustering of events over a wide range of scales, has also been used across many disciplines. It has been applied to a two-dimensional spatial area with univariate data to study the spread of disease (Carslake *et al.* 2005), plant distributions (Haase 1995, Podani and Czárán 1997, Dale 1999), and crime incidence (Levine 2005), and on one-dimensional lengths to measure clustering of animal–vehicle collisions (Clevenger *et al.* 2003, Ramp *et al.* 2005) along roads. Okabe and Yamada (2001) have adjusted the *K*-function algorithm to use bivariate data for network analysis, and Spooner *et al.* (2004) applied it to measure the interaction of plant species along roadsides. Analysis of bivariate data, namely, space–time clustering, with the *K*-function, is commonly used by medical and veterinary epidemiologists (e.g. Wilesmith *et al.* 2003, Carslake *et al.* 2005, Bastin *et al.* 2007) to statistically verify whether the time a collision occurs is dependent on where a collision occurs. It is an interesting measure as it provides an estimate of the increased risk associated with a collision due to clustering in time and space (Diggle *et al.* 1995), and has not yet been applied to study the excess risk of wildlife–vehicle collisions due to a space–time interaction. In our study, we used the *K*-function to measure statistical clustering of MVCs along roads with univariate space and time data and bivariate space–time data combined. Further methodologies and applications for spatial point pattern analysis are available in several books (e.g. Diggle 2003, Fotherhingham *et al.* 2000, O'Sullivan and Unwin 2003).

3. Exploratory analysis: kernel density estimation

This section presents results and discussion for the application of the kernel algorithm in space and time separately and then space and time together for MVCs on each road. Since the number of MVCs that occurred within each month on each

Downloaded By: [Syracuse University] At: 19:35 26 October 2009

road was low, the data were grouped together for all roads combined for our temporal analyses.

3.1 *Kernel density results*

3.1.1 Univariate kernel density estimation: space. We applied a kernel density (KD) estimator in one-dimensional space (i.e. road length) by varying the bandwidth (τ_s) from 2, 4, 6, and 10 km on each road. The number and magnitude of major peaks decreased and became more spread out as the bandwidth increased (Figure 4). We selected τ_s=4 km for interpretation because it measured density of collisions at an appropriate scale from a transportation and mitigation planning perspective along each road. The highest peak was recorded on VT-114N (τ_s=2 km, >6) and a smaller collision density peak was on VT-114S (Figure 4a and b). Highway VT-114N had three major peaks, VT-114S had two, and VT-105 and US-2 both had one large spread out peak.

3.1.2 Univariate kernel density estimation: time. For the kernel application in the temporal dimension, we varied the bandwidth for time (τ_t) at 4, 6, 12 and 24 months. As the bandwidth increased, the crests became more smooth (Figure 5). Data beyond 1999 are not deemed representative of the long-term trend, due to a combination of increased hunting, a decrease in sampling effort and a time lag for

Downloaded By: [Syracuse University] At: 19:35 26 October 2009

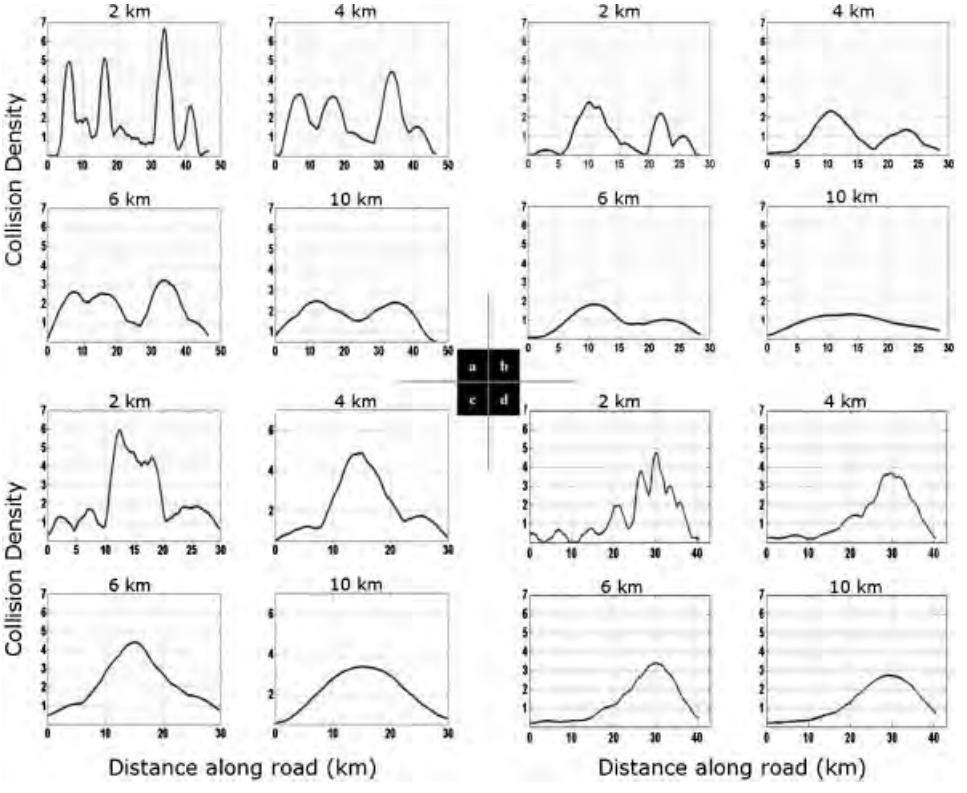

Figure 4. Kernel density estimation for a) VT-114N, b) VT-114S, c) US-2, and d) VT-105. Kernel bandwidth increased for each road from 2, 4, 6 and 10 km. The crests represent relatively high densities of MVCs at that location $\pm$ the search distance (km).

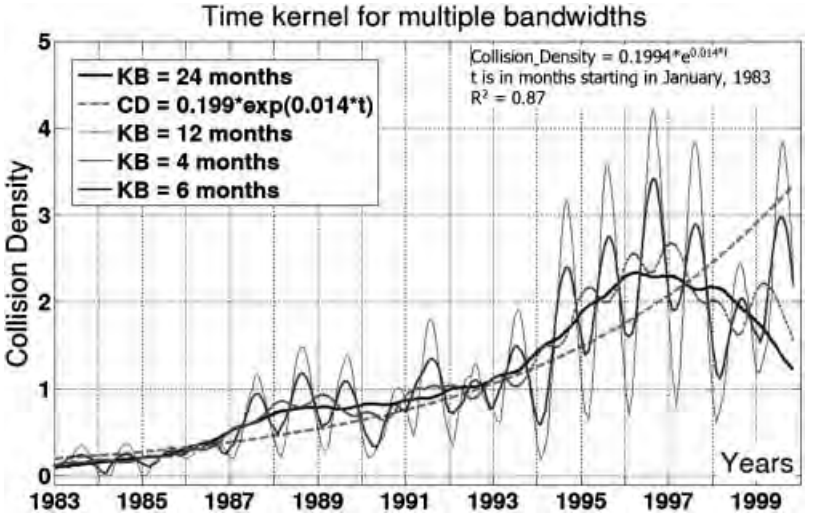

Figure 5. Kernel density estimation for time for all roads combined from January 1983 to October 1999 with variable kernel bandwidth (KB) 4, 6, 12 and 24 months. Figure also shows our interpolated (on 24 month KB) exponential increase in density (dashed gray line, $R^2=0.87$).

data input into the database (VAOT, personal communication). Therefore, we focused our trend fit until 1997 that includes data up to 1999 (1997 ± 24 month bandwidth). We used a bandwidth τ_t of 24 months (solid black line, Figure 5) to fit a simple exponential model (equation (9)) to identify the large-scale trend in collision density between months (with zero at January, 1983). The fitted function ($R^2=0.87$), is presented with a dashed gray line in Figure 5.

$$\text{Collision Density} = 0.1994e^{0.014t} \tag{9}$$

For interpretation, we selected a kernel bandwidth of $\tau_t=4$ months because it had clearly defined annual periodicity (i.e. each crest spread across 1 year), while simultaneously expressing the large-scale exponential increase (Figure 5). The highest density at $\tau_t=4$ months was 4.2 collision density at approximately August 1996. From the 17 annual peaks, 11 occurred in July, five in August and one in May. Therefore, at $\tau_t=4$ months, the highest peak of collisions occurred 65% of the time in July, which suggests high collision density from March to November (July ± 4 months).

3.1.3 Bivariate kernel density estimator: space and time interaction. To display the variation in combined intensities at various spatiotemporal scales, we selected four combinations of bandwidths for space and time [τ_s (km), τ_t (month)], namely, [2 km, 4 months], [2 km, 12 months], [4 km, 4 months] and [4 km, 12 months]. As τ_s and τ_t increased, the moderate to high density areas became more spread out and less discrete in space and time for the four combinations of bandwidths on each of the four roads (Figure 6).

Density measures for each two-dimensional kernel cell center had few MVCs in the first 5 years on all roads, i.e. collision density values $\leqslant 1$ (white or light gray), except VT-114N (Figure 6a). Moderate intensities (~ 2 collision density) were recorded on VT-114N from approximately 30 to 35 km, and July 1987 to October

Downloaded By: [Syracuse University] At: 19:35 26 October 2009

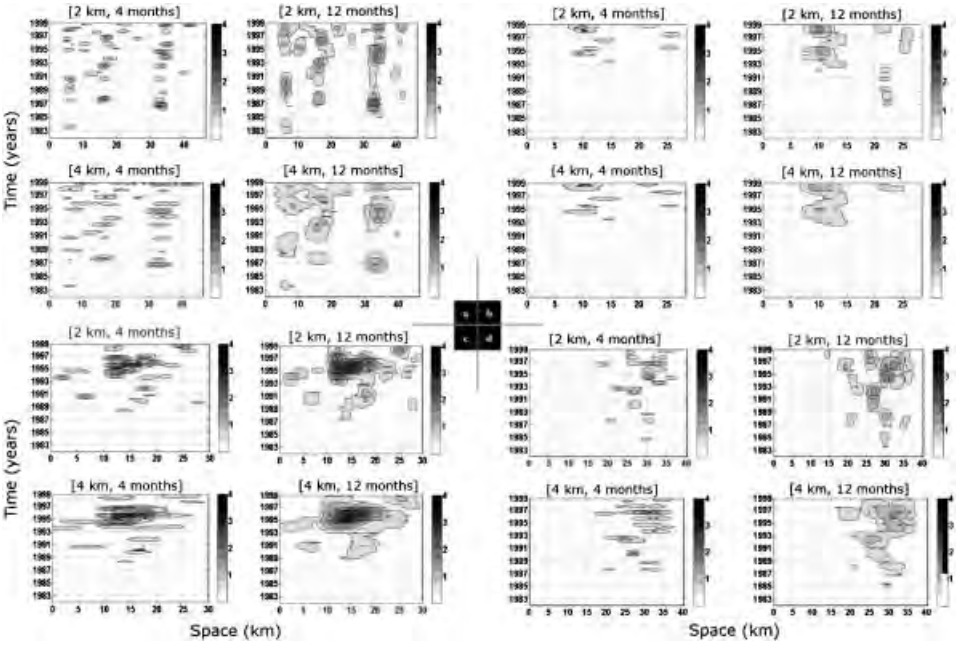

Figure 6. Bivariate kernel space and time moose-vehicle collision densities for a) VT-114N, b) VT-114S, c) US-2, and d) VT-105, with bandwidth combinations [τ_s (km), τ_t (month)] at [2 km, 4 months], [2 km, 12 months], [4 km, 4 months] and [4 km, 12 months].

1988, and again from approximately November 1994 to June 1996 (Figure 6a). VT-114S had one moderate density area at approximately 10 km in 1999, and low density in the 1980s corresponding to very few collisions occurring in this time period (Figure 6b). Road VT-105 had one large moderate area from approximately 25 to 35 km and from October 1993 to January 1999 (Figure 6d). Road US-2 had the highest density (3.2) for the largest spatiotemporal extent, from approximately 10 to 20 km from June 1995 to December 1997 (Figure 6c).

With the addition of the temporal dimension, the density in space was occasionally separated into discrete temporal periods. For example, at [4 km, 12 months], VT-114N displayed moderate densities in 1987 and not again until 1994 (Figure 6a). Most notable was the spatiotemporal pattern on VT-105 at a search combination of [2 km, 12 months] (Figure 6d), which showed continuous peaks of low to moderate density spanning from 1987 to 1999; however, these clusters shifted spatially through time. Moderate intensities first centered at 30 km from 1984 to 1989, then at 25 km from 1989 to 1993 and then spread across 30 to 35 km from 1993 to 1999.

3.2 *Kernel density discussion*

3.2.1 Univariate kernel density estimator: space. One of the major challenges associated with using the kernel estimation is the bandwidth selection for the analysis. This is a critical step in any application of kernel estimation, which requires testing and knowledge of the spatial and temporal distribution of the events being described. Our selection of a spatial bandwidth at 4 km to interpret our results was further justified, as we will demonstrate later, with the Ripley's K analysis. The

Downloaded By: [Syracuse University] At: 19:35 26 October 2009

spatial extent of the major peaks in Figure 4 was similar to the peak clustering scale in the Ripley's *K* analysis for each road (Figure 8). Krisp and Durot (2007) selected 2 km as a suitable bandwidth to apply the kernel estimation to moose collision data for optimal placement of wildlife signage; however, this was determined by consultation with the Finnish transportation authority and not by quantitative methods. In addition, a study by Clevenger *et al.* (2003), found clustering of animal collisions on roads at similar scales, e.g. 2 km for birds and 4 km for small mammals.

Previous studies have shown that in most cases, collisions with wildlife are not spatially random but are aggregated due to habitat type and terrain surrounding roads (Clevenger *et al.* 2003, Ramp *et al.* 2005). The kernel analyses in our study, which showed the scale and distribution of major peaks along the road, can assist in determining the potential spatial factors which are contributing to aggregated patterns of MVCs. For example, if preferred habitat elements for moose, such as wetlands, marsh-lands and moist coniferous forests (Markgren 1974; Bergstrom and Hjeljord 1987, Cederlund and Okarma 1988), are surrounding road segments where a high density of collision occur, this would support their inclusion in statistical models that predict factors associated with moose collisions (Seiler 2005, Dussault *et al.* 2007).

3.2.2 Univariate kernel density estimator: time. The kernel density function was in essence a weighted moving average and calculated the density of successive, overlapping groups of observations along a time line. As the bandwidth (months) increased, there was a smoothing effect which dampened out the fluctuations in the time series, allowing the more systematic components to be viewed (Burt and Barber 1996). The exponentially increasing large-scale trend from 1991 to 1996 in the time series at a bandwidth of 24 months follows an exponential rate of increase, similar to the non-linear increase in moose population in Vermont (i.e. 200 animals in 1980 to over 4000 animals in 2006) (Vermont Department of Fish and Wildlife, personal communication).

The collision density in time also showed recurring annual periodicity fluctuating above and below the main exponential trend existent in the data. The annual periodicity showed collisions rising steadily from January, peaking in July or August, and steadily decreasing until December. This seasonality has been documented in other regions in northeastern North America where the majority of moose collisions occurred between May and October (Joyce and Mahoney 2001, Dussault *et al.* 2007) and has been related to moose reproductive and behavioral patterns. The increase in food availability during the spring green-up and summer growing season would attract moose to the wetland forest complexes, especially along roads due to the high abundance of salty wetland plants. Further, there is often an increase in vehicle collision rates with subadult and yearling moose during the summer and autumn months due to the increased mobility of cows, or because cows are involved in mating (Peterson 1955, Cedurland *et al.* 1987).

3.2.3 Bivariate kernel density estimator: space and time interaction. This analysis demonstrated that the combination of space and time densities was more powerful than an independent investigation of space or time. We identified peak intensities from 1990 to 1996 (with the exception of VT-114S) on all roads (Figure 6). This can be explained by a concurrent dramatic increase in moose population abundance (Vermont department of Fish and Wildlife 1998); however, on VT-114N and VT-105 there were short peak intensities in the 1980's when moose numbers were low.

Downloaded By: [Syracuse University] At: 19:35 26 October 2009

This suggests that other short-term dynamic factors are influencing collisions at these locations, possibly variable traffic volume. Furthermore, different weather patterns such as increased snowfall and varying temperatures may change the number of moose–vehicle and moose–train collisions from one year to the next (Dussault *et al.* 2007, Gundersen *et al.* 1998).

Collision hotspots were not stationary but shifted spatially along some roads through time, and we identified several discontinuous periods of hotspot collisions. This is emphasized in Figure 7 that explicitly shows the spatiotemporal gap where no MVCs occurred as seen earlier in Figure 6d. This gap would not have been detected if space and time had been looked at separately (outlying x and y graphs on Figure 7). A possible explanation for this spatiotemporal shift may be a change in the foraging conditions near roads. For example, the location and proximity of brackish salt pools at roadside habitat, which has been shown to attract moose to roadsides and contribute to increased collisions (Dussault *et al.* 2007).

Downloaded By: [Syracuse University] At: 19:35 26 October 2009

4. Multi-scale statistical analysis: Ripley's *K*-function

One of the limitations of the kernel density method is that it does not provide a statistical estimate for the bandwidth size. Our conclusion from the kernel exploration is that clustering exists in space, time and space–time. Selection of specific bandwidth for the kernel function in space or in time depends on the user's perspective, i.e. the scale they would like to support. Furthermore, the kernel method allows us to explore the observed patterns; however, it does not clearly define an estimation of the clustering magnitude in a statistical manner. In this section, we provide the statistical verification of our initial exploratory kernel analyses using modified Ripley's K statistics. The collision dataset had a spatial accuracy of ± 800 m and a temporal accuracy of ± 1 day.

Another advantage of the Ripley's K analysis is its robustness to spatial error (± 800 m) and temporal error (± 1 day) in our data set, when compared to the

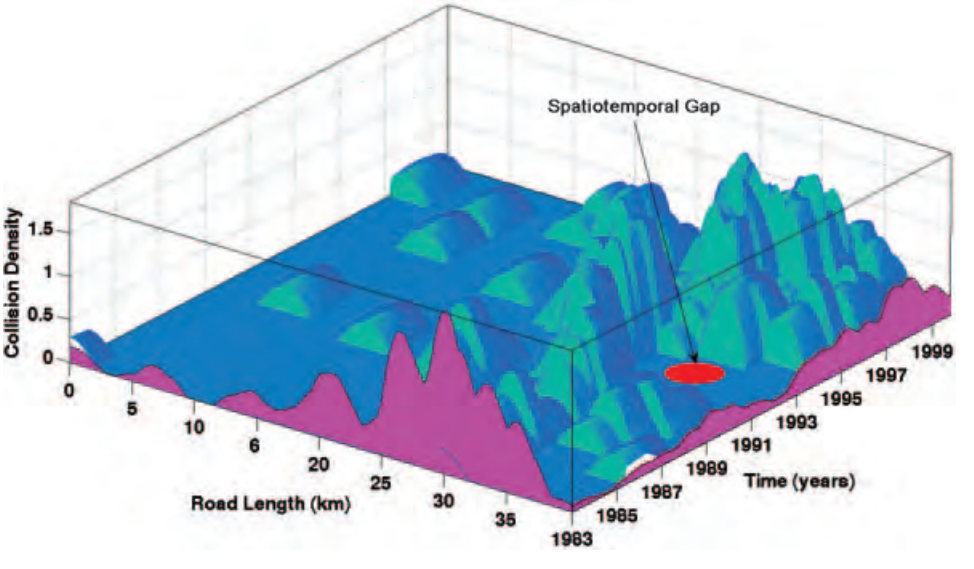

Figure 7. Space (bandwidth = 2km), time (bandwidth = 12 months) and space-time interaction (bandwidth = [2 km, 12 months]) kernel results for road VT-105.

Kernel method. The Ripley's K method uses all points for each analysis on each road, while the kernel method analyzes only specific segments of a road that fall within the search radius of the bandwidth. Therefore, assuming a random distribution for the spatial error, such an error will not have a significant affect in the overall Ripley's K analyses assuming that we look for clustering at scales beyond the spatial and temporal errors of the dataset.

We statistically tested for clustering evidence by assessing the significance of departure of the observed Ripley's $K(s)$ and $K(t)$ functions from complete spatial and temporal randomness at multiple scales. We generated 1000 Monte Carlo random simulations of an equivalent number of MVCs in space and time and computed the K- (equations (2) and (3)) and L-functions (equations (4) and (5)) for each simulation. We used Monte Carlo testing to rank the observed value amongst a set of values generated by random sampling (Besag and Diggle 1977). We then constructed 95% confidence envelopes to identify a statistical upper and lower range of complete randomness to compare with our observed distribution. If the observed L-function values were within the upper and lower limits (confidence envelopes), we assumed that the MVCs were randomly distributed. Any values of L that lied outside the upper confidence envelope were significantly clustered and any values that lay below the lower confidence envelope exhibited regularity at that scale distance. In order to limit the influence of edge effects on our calculated L values, we calculated the mean L for the 1000 random simulations and subtracted it from the observed L distributions and corresponding confidence envelopes.

We first describe the results and then the discussions of the spatiotemporal univariate and bivariate Ripley's K-function analyses. We look at each road separately for space, time and space–time analyses.

4.1 *Ripley's K-function results*

4.1.1 Univariate K-function: space. For the K-function space analysis, we increased the scale distance by increments of 500 m (step size). For relative comparisons between roads, clustering is referred to as the deviation of the observed L values from the upper 95% envelope and not the absolute peak in the observed function.

Peak clustering occurred at scale distances of 2.5 and 30 km for VT-114N, and at 5 and 15 km for VT-114S (Figures 8a and b). Road US-2 showed significant clustering at peak scale distances from 5 to 15 km (Figure 8c). Road VT-105 had the highest statistically significant deviation from spatial randomness, with peak clustering at a spatial scale distance of 10 km (Figure 8d). For both US-2 and VT-105, significant clustering was more spread out along each scale distance, corresponding to the major peaks in density seen in the kernel estimations for these same roads (Figures 4c and d). The deviation of peak clustering from randomness was highest on VT-105 ($\sim$4.5) as compared to the other roads ($\sim$1.5).

4.1.2 Univariate K-function: time. For the K-function time analysis, we increased the scale distance by increments of 1 month (step size) to investigate both annual periodicity and the exponential large-scale trend. Road VT-114N had significant clustering up to a scale distance of 9 years after which clustering was only significant during annual peak months. The first peak in clustering was at a scale distance of 3 months and is reached again approximately every 12 months thereafter (Figure 9a). Since the algorithm searches for MVCs within the scale distance symmetrically from both sides of the collision, significant clustering of MVCs occurred within a 7 month

Downloaded By: [Syracuse University] At: 19:35 26 October 2009

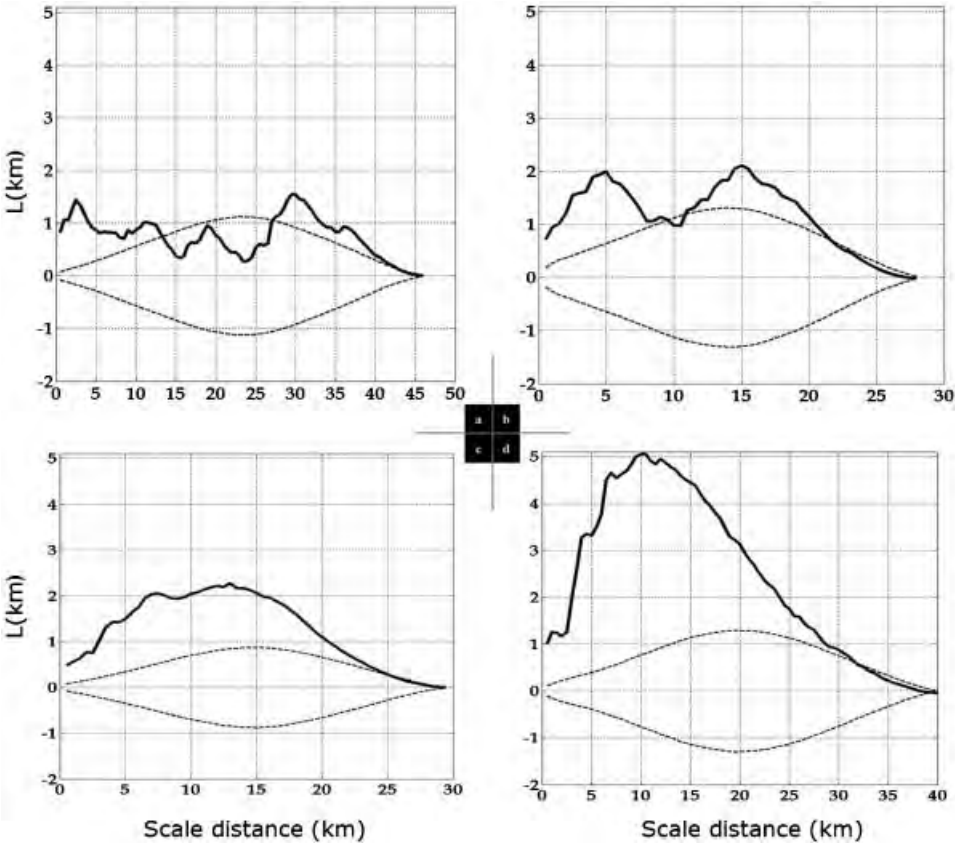

Figure 8. Plots of the observed $L(s)$ (solid thick line) with 95% confidence envelopes (dotted lines) as a function of scale distance for the distribution of MVCs on four roads: a) VT-114N, b) VT-114S, c) US-2, d) VT-105. Observed values above the upper confidence envelope indicate spatial clustering.

Downloaded By: [Syracuse University] At: 19:35 26 October 2009

period (1 ± 3 months scale distance), similar to the periodicity results from the kernel investigation. Road VT-114S showed peak clustering between 5 and 7 years and this was approximately a three-fold increase in clustering as compared to VT-114N (Figure 9b). Significant clustering was the highest for US-2, peaking at 3–5 years and occurring at almost all temporal scales (Figure 9c). Road VT-105 exhibited clustering across most temporal scale distances, most significantly up to 4 years (Figure 9d). Peak clustering on all roads occurred at an approximate scale distance of 5 years similar to the high densities seen in MVCs from 1993 to 1999 in the space–time kernel estimation (Figure 6).

4.1.3 Bivariate K-function: space and time interaction. We used a normalized index $D_o(s, t)$ (equation (8)) to express the proportional excess of clustering due to a space–time interaction versus an added contribution from space and time separately. We first investigated evidence of interaction over large scales by visualizing the $D_o(s, t)$ metric at spatial scales up to 15 km (x axis) and temporal scales up to 15 years (y axis). Space–time interaction was not evident beyond 5 km and 5 years; therefore, we focused on the space–time interaction by plotting the $D_o(s, t)$ metric at spatial scales up to 5 km and temporal scales up to 5 years (Figure 10). At these scale distances,

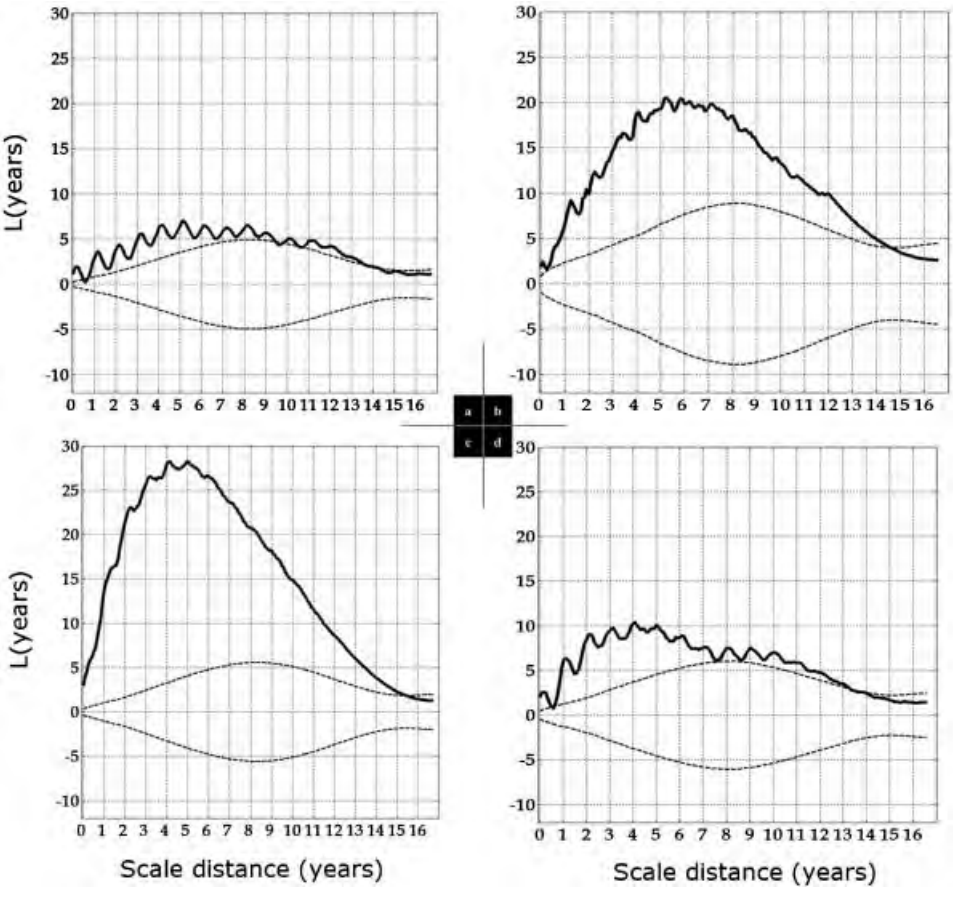

Figure 9. Plots of the observed $L(s)$ (solid thick line) with 95% confidence envelopes (dotted lines) as a function of scale distance for the distribution of MVCs on four roads: a) VT-114N, b) VT-114S, c) US-2, d) VT-105. Observed values above the upper confidence envelope indicate temporal clustering.

the $D_o(s, t)$ metric was the highest on US-2 at 0.82 (Figure 10c) relative to the other roads where proportions were smaller at 0.65. In addition to relatively high space–time interaction (>0.2) for small spatial (up to 2.0 km) and temporal (up to 3.0 years) scales, US-2 exhibited interaction at larger spatial scales (3–5 km) up to temporal scales of 1.5 years. At the 2–3 km spatial scale, space–time clustering was minimal.

Road VT-114S displayed a unique distribution of space–time interaction. At temporal and spatial scales up to 1 year and 1 km, space–time clustering is present (Figure 10b). However, that trend did not continue at spatial scales between 1 and 2 km, where the interaction is clearly dependent on the temporal scale. For small temporal scales up to 6 months, there is no space–time interaction, but when temporal scales increased from 6 months to 1 year and again after 3.5 years, there is evidence of space–time dependency. At larger spatial scales (2–5 km), interaction is more evident up to 1 year, but moderately exists up to 5 years.

Road VT-114N (Figure 10a) exhibited much different behavior than VT-114S. Space–time interaction was restricted to small temporal (up to 2 years) and spatial

Downloaded By: [Syracuse University] At: 19:35 26 October 2009

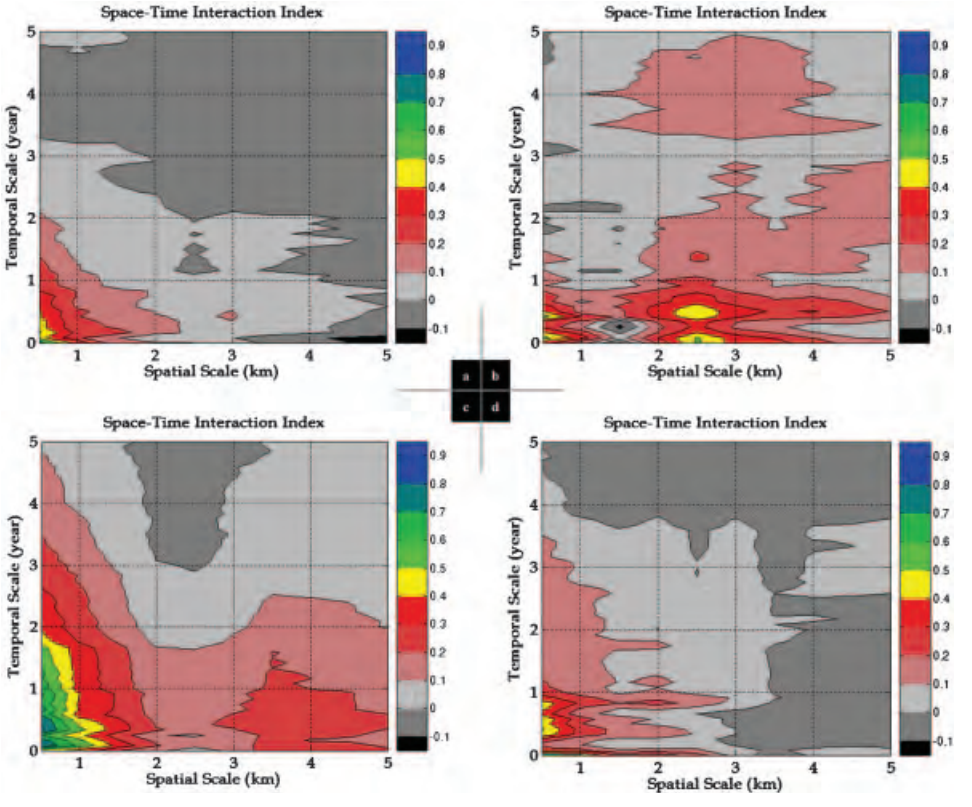

Figure 10. Contour plots of the $D_o(s, t)$ at temporal scales up to 5 years and spatial scales up to 5 km on a) VT-114N, b) VT-114S, c) US-2, d) VT-105. $D_o(s, t)$ is the proportional increase, or excess risk, attributable to space-time clustering.

scales (up to 2 km). Road VT-105 (Figure 10d) was similar to VT-114N with observed clustering up to slightly larger spatial and temporal scales.

4.2 *Ripley's K-function discussion*

4.2.1 Univariate K-function: space. The Ripley's *K*-function emphasized the variation in spatial scale and magnitude at which MVCs were distributed and varied on each road. Significant clustering was heavily spread out, peaking at approximately 12 km on US-2 and VT-105 suggesting that collisions are influenced by environmental variables at large spatial scales. Since both these roads had higher annual average daily traffic volumes (>2400) than VT-114 (<1600), this may have contributed to a larger risk of collisions along greater stretches of road creating more uniform patterns (clustering at extended spatial scales).

Similar to the results in the kernel analysis, the identification of significant clustering scale will assist in determining which spatial features surrounding roads are influencing the occurrence of collisions. The juxtaposition of landscape elements surrounding roads will act as corridors or barriers to a particular animal's movement (Forman and Godron 1981) and therefore will influence the location and scale of collisions. For example, significant clustering of MVCs at scale distances smaller than 10 km may be attributed to the spatial extent and configuration of habitat elements which may also occur at this scale surrounding the road.

Downloaded By: [Syracuse University] At: 19:35 26 October 2009

4.2.2 Univariate K-function: time. Each road showed similar peak scales (5 years) in temporal clustering providing statistical evidence that the collisions between 1993 and 1999 were different than random. The deviation from the upper confidence envelope contrasted greatly between roads, for example, US-2 and VT-114S showed much higher clustering than the other two roads. An increase in collisions in the 1990s combined with few to no collisions in the 1980s would have caused the drawn out pattern of significant clustering on these roads (see kernel space–time in Figure 6). Furthermore, the annual periodicity was more evident on VT-114N and VT-105 which suggests a more consistent long-term seasonal trend for collisions on these roads. Comparisons between roads should be interpreted with caution because there may have been a human bias in MVC sampling on each road. Further, long-term consistent data collection on all roads could tease out the variations in temporal trends due to human bias or from other collision factors such as traffic volume.

4.2.3 Bivariate K-function: space and time interaction. Our results provide evidence that an excess risk in collisions is due to the interaction of where and when a collision occurs at small spatial and temporal scales. In previous studies, scientists have shown that collisions with wildlife are clustered in time (Joyce and Mahoney 2001), and in space (Clevenger *et al.* 2003, Ramp *et al.* 2005) due to various environmental factors. The varied scales at which space–time interactions occur on each road suggest that a combination of these factors is influencing the collisions differently on each road. For example, moose disperse and migrate seasonally to optimize food availability (Franzmann and Schwartz 1997), and more specifically in our study area, moose commonly move from higher elevation wintering grounds with more mature mixed woods to large wetlands, or marsh-lands in the spring (Vermont Fish and Wildlife, personal communication). Our selected roads in the highlands may or may not bisect the movement path between winter and summer feeding areas, influencing collision rates differently during specific periods of animal movements.

Downloaded By: [Syracuse University] At: 19:35 26 October 2009

5. Collective thoughts and implications for mitigation strategies

The motivation behind our work was to analyze the spatial and temporal locations and extent for MVCs in order to provide effective mitigation strategies. Our hypothesis that MVCs are clustered in space, time and space–time was verified through our analyses. We combined our significant spatiotemporal findings and discussions from both the kernel and Ripley's analyses and provided a plausible mitigation strategy using a planning rubric in Table 1 below. This table is targeting mitigation planners rather than spatial scientists; therefore, we converted our quantitative results into qualitative summary metrics. It should be viewed more as a comparative guide for the investigated roads rather than as an absolute metric of behavior for each road independently. In all comparisons using Ripley's K results, the scale distances are symmetrical along the road at each MVC, for example, a 2 km spatial scale would correspond to a 4 km long road segment.

The spread and magnitude of the major peaks in the kernel density analysis on each road can assist transportation planners in determining the scale to apply a mitigation strategy. Furthermore, the spread and magnitude of the major peaks in the kernel density analysis on each road are complemented with the clustering results in the Ripley's K analysis. For example, VT-105 and US-2 both had major density peaks which spread across approximately 10–30 km of road, while the Ripley's K analysis showed significant peak clustering at similar road scales,

Downloaded By: [Syracuse University] At: 19:35 26 October 2009

Table 1. Mitigation strategy rubric. A summary of obtained results from spatial and spatiotemporal Kernel density and Ripley's *K* analyses and implications for appropriate mitigation strategies.

Road	Peak location[a] (KS)	Density[a] (KS)	Spread of peaks (KS)	Peak clustering scale[b] (RS)	Cluster intensity[c] (RS)	Spatiotemporal gap presence[d] (KST)	Spatiotemporal interaction[e] (RST)	Mitigation strategy		
								Need[f]	Suggestion[g]	Confidence[g]
VT-114N	6th km	Medium	8 km	3 km	Medium	Yes	Low	Medium	Temporary	High
VT-114N	16th km	Medium	8 km			No		Medium	Temporary	Low
VT-114N	34th km	High	10 km			No		High	Permanent	High
VT-114S	11th km	Medium	12 km	5 km	Medium	No	High	Medium	Temporary	Low
VT-114S	23rd km	Low	7 km			Yes		Low	Temporary	High
US-2	14th km	High	14 km	4–15 km	Medium	Yes	High	High	Permanent	Low
VT-105	30th km	Medium	30 km	4–15 km	High	Yes	Medium	High	Permanent	Low

KS=Kernel space, RS=Ripley space, KST=Kernel space–time, RST=Ripley space–time. All numbers rounded to the nearest integer.
[a]Expressed as Low [<2], Medium [2, 4] and High [>4] using the 4 km bandwidth kernels (Figure 4).
[b]Identified using the Ripley's *K*-function in space (Figure 8).
[c]Measured as the deviation from randomness, expressed as Low [<1], Medium [1, 3] and High [>3] (Figure 8).
[d]Measured by the repeated presence of collisions through time for each peak location. If collision density shifted spatially along a road or collision density exhibited a temporal lapse (>1 year), a spatiotemporal gap was present (Figure 6).
[e]Ripley's K-function for spatiotemporal interactions (Figure 10) was inspected and ranked as Low, Medium and High based on spread of interaction. Lower ranking would lead to higher confidence for permanent strategies because well defined locations in space and time exist for placement of crossing structures.
[f]The need for a mitigation strategy based on relative density of collisions (KS) and clustering intensity (RS). Low derived from low and medium scores, Medium derived from two medium scores, and High derived from medium and high KS and RS scores.
[g]Temporary and less expensive measures (e.g. wildlife signage) were recommended for road segments where the need was ranked as medium or low, and/or a spatiotemporal gap was present. High confidence was given if a spatiotemporal gap is present. Permanent and more expensive strategies (e.g. crossing structure and fencing) were recommended for road segments where the need ranked medium to high and stronger confidence was given if collision density in space was consistent through time (no spatiotemporal gaps and low spatiotemporal interaction).
Note: The above table should be used as a general comparable guide prioritizing mitigation efforts within our study area. Quantitative measures were converted to qualitative metrics using reasonable but nonetheless objective thresholds.

4–15 km (e.g. $4 \times 2 = 8$ km and $15 \times 2 = 30$ km road segment hotspots for VT-105 and US-2) (Table 1). Additionally, roads VT-114N and VT-114S both showed more concentrated peaks spread out at 8 and 10 km respectively that was verified by the Ripley's *K*-function with significant clustering peaking at a spatial scale of approximately 3 and 5 km respectively (Table 1).

A difficult question for transportation mitigation planning is whether the collisions will reoccur at the same scale and intensity for prolonged periods to justify the need for more permanent, expensive structures. We took this into account when providing a plausible mitigation strategy (permanent versus temporary) for each road separately (Table 1). Permanent strategies (e.g. wildlife crossing structures and fencing, see example in Clevenger and Waltho 2000), have proven to be very effective and have reduced wildlife–vehicle collisions for ungulates by at least 80% (Clevenger *et al.* 2001); however, they are typically the most costly scenario. A temporary mitigation strategy is less costly, such as the use of wildlife signs, and public awareness campaigns, and it is more effective if spatiotemporal periods are known (Huijser *et al.* 2007).

Our mitigation recommendations are based on relative comparisons between roads and therefore assume that all roads were sampled with the same effort. In addition, we do not use any criteria that is documented in the literature set by transportation agencies. Finally, our suggestions are preliminary and we were conservative when suggesting deployment of permanent costly measures to reflect limited budgets, typical of most transportation agencies.

Looking at each road separately, a plausible mitigation strategy for VT-114N may be to deploy multiple permanent crossing structures with associated fencing at each of the three major peaks. However, a more feasible option may be a permanent structure at 34 km where collisions were consistent and high, and temporary measures at the other two peaks (6 and 16 km). Road VT-105 showed high clustering intensity justifying a permanent strategy; however, the spatial scale of collisions was high making it difficult to place or justify only one permanent structure along the length of road. Furthermore, the spatiotemporal shift evident in collision intensity warrants further investigation to determine the correct placement of a crossing structure. Fencing could be used to funnel animals into the crossing structure if the spatiotemporal shift in collisions is within a manageable scale. Although US-2 had a clear spatiotemporal gap, the kernel density analyses identified this road with the highest densities of collisions in space and time. The collisions increased or spread across a larger road segment through the temporal period studied. Considering the above, we would suggest further research to investigate the spatiotemporal gaps before implementing a permanent, costly strategy for this road. Finally, temporary measures are recommended for the two peaks on road VT-114S because cluster density and intensity were ranked low or medium. Both peaks exhibited dynamic spatiotemporal patterns in both the kernel and Ripley's spatiotemporal analyses that may possibly be linked to the low sample size for that road (51 MVCs). Therefore, only temporary mitigation measures are suggested, however more data collection and research may justify with confidence the need for more permanent measures.

The diversity of the mitigation planning strategies aforementioned is partly due to the dissimilar spatiotemporal patterns of MVCs on each of our four roads. We provide further evidence for this by displaying the average and standard deviation values for space-time interaction at all scales for all four roads combined (Figures 11 and 12). Overall, the spatiotemporal clusters appear at smaller spatiotemporal scales; however, the standard deviation (Figure 12) shows that the intensity is highly

Downloaded By: [Syracuse University] At: 19:35 26 October 2009

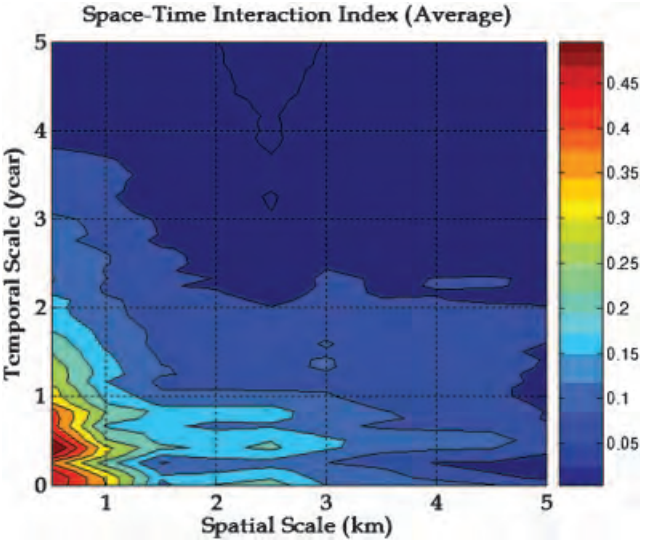

Figure 11. Average space-time interaction for all roads.

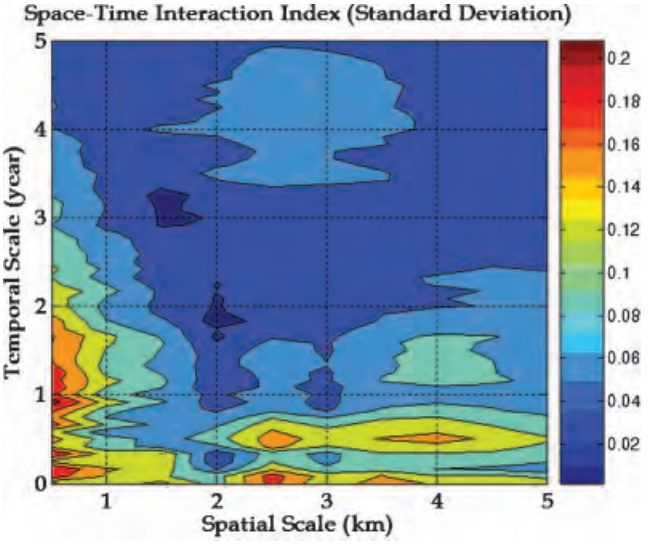

Figure 12. Variability in space-time interaction between all roads.

variable between roads at small and large spatiotemporal scales when the temporal scale is below 2 years.

6. Conclusion

We used an adapted kernel density estimator and Ripley's *K*-function for exploratory and multi-scale statistical analyses to determine the spatiotemporal patterns of MVCs along different road segments. In retrospect, using multiple roads proved effective to display varying and similar spatiotemporal patterns on roads. Additionally, the use of two algorithms (kernel and Ripley's *K* function)

Downloaded By: [Syracuse University] At: 19:35 26 October 2009

complemented and supplemented our results for each implementation. Furthermore, the bivariate spatiotemporal analyses provided unique results, not apparent in our univariate analyses, namely, whether collisions exhibit static or dynamic behavior at specific locations. Lastly, our methods are easily transferable to other roads where datasets are consistently collected in space and time.

7. Future work

In this study, we identified spatiotemporal clusters of MVCs. Positive space–time interaction indicates that a combination of spatial and temporal factors needs to be *dynamically* modeled to adequately predict where and when collisions will occur. The next logical step is to establish linkages between collision occurrence in space and time, and animal/vehicle movement patterns using information on the surrounding landscape (e.g. slope, vegetation), road characteristics (e.g. speed limit) and other dynamic movement factors (e.g. weather). For example, it would be interesting to relate where, when and how long moose migration patterns occur in the northeastern highlands of Vermont and link this to the spatiotemporal patterns we observed on the four roads. Such modeling would lead to increased prediction capabilities allowing for improved planning for future mitigation strategies. Finally, the collection of accurate (using Global Positioning Systems) and consistent wildlife–vehicle collision data over prolonged time periods will support spatiotemporal modeling at finer spatial resolutions.

Downloaded By: [Syracuse University] At: 19:35 26 October 2009

Acknowledgements

This project was partially funded by a SUNY-ESF Graduate Assistant award, and a grant from the US human society. We would like to thank the Vermont Agency of Transportation and the Department of Fish and Wildlife namely John Austin, Kevin Viani and Cedric Alexander, for collating the moose collision dataset and providing information during the analyses. We also greatly appreciate the thoughtful comments from the reviewers that improved the readability of the manuscript.

References

Austin, J.K., Viani, F. and Hammond, F., 2006, *Vermont Wildlife Linkage Habitat Analysis* (Burlington, VT: Vermont Department of Fish and Wildlife Service).

Bailey, T.C. and Gatrell, A.C., 1995, *Interactive Spatial Data Analysis* (Essex: Longman Scientific and Technical).

Bastin, L., Rollason, J., Hilton, A., Pillay, D., Corcoran, C., Elgy, J., Lambert, P., De, P., Worthington, T. and Burrows, K., 2007, Spatial aspects of MRSA epidemiology: a case study using stochastic simulation, kernel estimation and SaTScan. *International Journal of Geographical Information Science*, **21**, pp. 811–836.

Bergstrom, R. and Hjeljord, O., 1987, Moose and vegetation interactions in Northwestern Europe and Poland. *Swedish Wildlife Research*, **Suppl. 1**, pp. 213–228.

Besag, J. and Diggle, P.J., 1977, Simple Monte Carlo test for spatial pattern. *Applied Statistics*, **26**, pp. 327–333.

Burt, J.E. and Barber, G.M., 1996, *Elementary Statistics for Geographers* (New York: Guilford Press).

Carslake, D., Bennett, M., Bown, K., Hazel, S., Telfer, S. and Begon, M., 2005, Space–time clustering of cowpox virus infection in wild rodent populations. *Journal of Animal Ecology*, **74**, pp. 647–655.

Cederlund, G. and Okarma, H., 1988, Home range and habitat use of adult female moose. *Journal of Wildlife Management*, **52**, pp. 336–343.

CLEVENGER, A.P. and WALTHO, N., 2000, Factors influencing the effectiveness of wildlife underpasses in Banff National Park, Alberta, Canada. *Conservation Biology*, **14**, pp. 47–56.

CLEVENGER, A.P., CHRUSZCZ, B. and GUNSON, K.E., 2001, Highway mitigation fencing reduces wildlife–vehicle collisions. *Wildlife Society Bulletin*, **29**, pp. 646–653.

CLEVENGER, A.P., CHRUSZCZ, B. and GUNSON, K.E., 2003, Spatial patterns and factors influencing small vertebrate fauna road-kill aggregations. *Biological Conservation*, **109**, pp. 15–26.

DALE, M.R.T., 1999, *Spatial Pattern Analysis in Plant Ecology* (Cambridge: Cambridge University Press).

D'ANGELO, G.J., D'ANGELO J.G., GALLAGHER, G.R., OSBORN, D.A., MILLER, K.V. and WARREN, R.J., 2006, Evaluation of wildlife warning reflectors for altering white-tailed deer behavior along roadways. *Wildlife Society Bulletin*, **34**, pp. 1175–1183.

DIGGLE, P.J., CHETWYND, A.G., HAGGKVIST, R. and MORRIS, S.E., 1995, Second-order analysis of space-time clustering. *Statistical Methods in Medical Research*, **4**, pp. 124–136.

DIGGLE, P.J., 2003, Statistical Analysis of Spatial Point Patterns (Oxford: Oxford University Press).

DUSSAULT, C., ROULIN, M., COURTOIS, R. and OUELLET, J.P., 2007, Temporal and spatial distribution of moose-vehicle accidents in the Laurentides Wildlife Reserve, Quebec, Canada. *Wildlife Biology*, **12**, pp. 415–426.

ENVIRONMENTAL SYSTEMS RESEARCH INSTITUTE (ESRI), 2005, *ArcMap GIS*, version 9.1 (Redlands, CA: ESRI).

FIEBERG, J., 2007, Utilization distribution estimation using weighted kernel density estimators. *Journal of Wildlife Management*, **71**, pp. 1669–1675.

FORMAN, R.T.T. and GODRON, M., 1981, Patches and structural components for a landscape ecology. *BioScience*, **31**, pp. 733–740.

FOTHERHINGHAM, A.S., BRUNSDON, C. and CHARLTON, C., 2000, *Quantitative Geography: Perspectives on Spatial Data Analysis* (London: Sage).

FRANZMANN, A.W. and SCHWARTZ, C.C., 1997, *Ecology and Management of the North American Moose* (Washington, DC: Smithsonian Institution Press).

GITZEN, R.A., MILLSPAUGH, J.A. and KERNOHAN, B.J., 2006, Bandwidth selection for fixed-kernel analysis of animal utilization distributions. *Journal of Wildlife Management*, **70**, pp. 1334–1344.

GROOT, G.W.T.A. and HAZEBROEK, E., 1996, Ungulate traffic collisions in Europe. *Conservation Biology*, **10**, pp. 1059–1067.

GUNDERSEN, H., ANDREASSEN, H.P. and STORAAS, T., 1998, Spatial and temporal correlates to Norwegian moose–train collisions. *Alces*, **34**, pp. 385–394.

HAASE, P., 1995, Spatial pattern analysis in ecology based on Ripley's *K*-function: introduction and methods of edge correction. *Journal of Vegetation Science*, **6**, pp. 574–582.

HUIJSER, M.P., MCGOWEN, P., FULLER, J., HARDY, A., KOCIOLEK, A., CLEVENGER, A.P., SMITH, D. and AMENT, R., 2007, Wildlife–vehicle collision reduction study. Report to Congress (Washington, DC: US Department of Transportation, Federal Highway Administration).

HUBBARD, M.W., DANIELSON, B.J. and SCHMITZ, R.A., 2000, Factors influencing the location of deer-vehicle accidents in Iowa. *Journal of Wildlife Management*, **64**, pp. 707–712.

JOYCE, T.L. and MAHONEY, S.P., 2001, Spatial and temporal distributions of moose–vehicle collisions in Newfoundland. *Wildlife Society Bulletin*, **29**, pp. 281–291.

KRISP, J.M. and DUROT, S., 2007, Segmentation of lines based on point densities – An optimisation of wildlife warning sign placement in southern Finland. *Accident Analysis and Prevention*, **39**, pp. 38–46.

LEVINE, N., 2005, *CrimeStat: A Spatial Statistics Program for the Analysis of Crime Incident Locations* (version 3.0) (Houston, TX: Ned Levine and Associates).

Downloaded By: [Syracuse University] At: 19:35 26 October 2009

MAINE DEPARTMENT OF TRANSPORTATION 2001, Collisions between large wildlife species and motor vehicles in Maine. Interim Report, pp. 33.

MARKGREN, G., 1974, The moose in Fennoscandia. *Naturaliste Canadien*, **101**, pp. 185–194.

MCGUIRE, T.M. and MORRALL, J.F., 2000, Strategic highway improvements to minimize environmental impacts within the Canadian Rocky Mountain National Parks. *Canadian Journal of Civil Engineering*, **27**, pp. 523–532.

MOSER, B.W. and GARTON, E.O., 2007, Effects of telemetry location error on space-use estimates using a fixed-kernel density estimator. *Journal of Wildlife Management*, **71**, pp. 2421–2426.

THE MATHWORKS 2005, *Matlab*, version 7.0 (Natick, MA: Mathworks).

OKABE, A. and YAMADA, I., 2001, The K-function method on a network and its computational implementation. *Geographical Analysis*, **33**, pp. 271–290.

O'SULLIVAN, D. and UNWIN, D.J., 2003, *Geographic Information Analysis* (Hoboken, NY: John Wiley & Sons).

PETERSON, R.L., 1955, *North American Moose* (Toronto, Ont.: University of Toronto).

PODANI, J. and CZARAN, T., 1997, Individual-centred analysis of mapped point patterns representing multi-species assemblages. *Journal of Vegetation Science*, **8**, pp. 259–270.

RAMP, D.J., CALDWELL, J., EDWARDS, K.A., WARTON, D. and CROFT, D.B., 2005, Modeling of wildlife fatality hotspots along the snowy mountain highway in New South Wales, Australia. *Biological Conservation*, **126**, pp. 474–490.

RAMP, D., WILSON, V.K. and CROFT, D.B., 2006, Assessing the impacts of roads in peri-urban reserves: road-based fatalities and road usage by wildlife in the Royal National Park, New South Wales, Australia. *Biological Conservation*, **129**, pp. 348–359.

RIPLEY, B.D., 1976, The second-order analysis of stationary point processes. *Journal of Applied Probability*, **13**, pp. 255–266.

RIPLEY, B.D., 1981, *Spatial Statistics* (Chichester: John Wiley & Sons).

ROMIN, L.A. and BISSONETTE, J.A., 1996, Deer–vehicle collisions: status of state monitoring activities and mitigation efforts. *Wildlife Society Bulletin*, **24**, pp. 276–283.

SAUER, T.M., BEN-DAVID, M. and BOWYER, R.T., 1999, A new application of the adaptive-kernal method: estimating linear home ranges of River otters, *Lutra Canandensis, Canadian Field Naturalist*, **113**, pp. 419–424.

SCHWABE, K.A., SCHUHMANN, P.W. and TONKOVICH, M., 2002, A dynamic exercise in reducing deer-vehicle collisions: Management through vehicle mitigation techniques and hunting. *Journal of Agricultural and Resource Economics*, **27**, pp. 261–280.

SEILER, A., 2004, Trends and spatial patterns in ungulate-vehicle collisions in Sweden. *Wildlife Biology*, **10**, pp. 301–313.

SEILER, A., 2005, Predicting locations of moose–vehicle collisions in Sweden. *Journal of Applied Ecology*, **42**, pp. 371–382.

SPOONER, P.G., LUNT, I.D., OKABE, A. and SHIODE, S., 2004, Spatial analysis of roadside *Acacia* populations on a road network using the network *K*-function. *Landscape Ecology*, **19**, pp. 491–499.

STEENBERGHEN, T., DUFAYS, T., THOMAS, I. and FLAHAUT, B., 2004, Intra-urban location and clustering of road accidents using GIS: a Belgian example. *International Journal of Geographic Information Science*, **18**, pp. 169–181.

THOMPSON, E.H., 2002, Vermont natural heritage: conserving biodiversity in the green mountain state. A report from the Vermont Biodiversity Project (Burlington, VT: Queen City Printers).

VERMONT DEPARTMENT OF FISH AND WILDLIFE. 1998, Moose management plan for the state of Vermont 1998–2007 (South Waterbury, VT: Vermont Department of Fish and Wildlife).

WILESMITH, J.W., STEVENSON, M.A., KING, C.B. and MORRIS, R.S., 2003, Spatiotemporal epidemiology of foot-and-mouth disease in two countries of Great Britain in 2001. *Preventive Veterinary Medicine*, **61**, pp. 157–170.

Downloaded By: [Syracuse University] At: 19:35 26 October 2009